Finite Temperature Lattice Properties of Graphene beyond the Quasiharmonic Approximation

K. V. Zakharchenko, M. I. Katsnelson, and A. Fasolino

Institute for Molecules and Materials, Radboud University Nijmegen, Heyendaalseweg 135, 6525 AJ Nijmegen, The Netherlands

(Received 15 December 2008; published 29 January 2009)

The thermal and mechanical stability of graphene is important for many potential applications in nanotechnology. We calculate the temperature dependence of the lattice parameter, elastic properties, and heat capacity by means of atomistic Monte Carlo simulations that allow us to go beyond the quasiharmonic approximation. We predict an unusual, nonmonotonic, behavior of the lattice parameter with a minimum at $T \approx 900$ K and of the shear modulus with a maximum at the same temperature. The Poisson ratio in graphene is found to be small ≈ 0.1 in a broad temperature interval.

DOI: 10.1103/PhysRevLett.102.046808 PACS numbers: 81.05.Uw, 62.20.−x, 65.40.De

Understanding the structural and thermal properties of two-dimensional (2D) systems is one of the challenging problems in modern statistical physics [1]. Traditionally, it was discussed mainly in the context of biological membranes and soft condensed matter. The complexity of these systems hindered any truly microscopic approach based on a realistic description of interatomic interactions. The discovery of graphene [2], the first truly 2D crystal made of just one layer of carbon atoms, provides a model system for which an atomistic description becomes possible. The interest for graphene has been triggered by its exceptional electronic properties (for a review, see [3–5]), but the experimental observation of ripples in freely hanged graphene [6] has initiated a theoretical interest also in the structural properties of this material [7,8]. Ripples or bending fluctuations have been proposed as one of the dominant scattering mechanisms that determine the electron mobility in graphene [9]. Moreover, the structural state influences the mechanical properties that are important in themselves for numerous potential applications of graphene [10–12].

Two-dimensional crystals are expected to be strongly anharmonic due to an intrinsic bending instability coupled to in-plane stretching modes. This coupling is crucial to prevent crumpling of the crystal and stabilize the flat phase [1]. These expectations have been confirmed by atomistic simulations for graphene showing very strong bond length fluctuations already at room temperature [7]. Beside the relevance for 2D systems, anharmonicity [13] is of general importance in condensed matter in relation to structural phase transitions [14,15], soft modes in ferroelectrics [16], melting [17], and related phenomena. Usually, anharmonicity in crystals is weak enough and thus can be well described in the framework of perturbation theory [13,18–20]. However, this might not be the case for strongly anharmonic systems, such as graphene. Atomistic simulations offer the possibility to study anharmonic effects for a specific material without the need of perturbative schemes. For carbon, a very accurate description of energetic and thermodynamic properties of different allotropes including graphene [7,21] is provided by the empirical bond order potential LCBOPII [22]. Here we present the temperature dependence of thermodynamical and elastic properties of graphene, calculated by means of atomistic Monte Carlo (MC) simulations based on LCBOPII.

We perform MC simulations at finite temperature T with periodic boundary conditions for a sample of $N = 8640$ atoms with an equilibrium size at zero temperature of 147.57 Å in the x direction and 153.36 Å in the y direction. We equilibrate the sample in the NPT ensemble at pressure $P = 0$ for at least 2×10^5 MC steps (1 MC step corresponds to N attempts to a coordinate change) which we found to be enough for convergence of total energy and sample size. Further, 10^5 MC steps are used to evaluate the average lattice parameter a, average nearest neighbor distance R_{nn}, and radial distribution function $g(R)$. The difference $(a - \sqrt{3}R_{nn})$ characterizes deviations from planarity.

Figure 1 shows that a and R_{nn} decrease with increasing temperature up to about 900 K, yielding a negative thermal expansion coefficient $\alpha = (-4.8 \pm 1.0) \times 10^{-6}$ K^{-1} in the range 0–300 K. As noted in Ref. [23], this anomaly is due to a low-lying bending phonon branch [24]. Our results

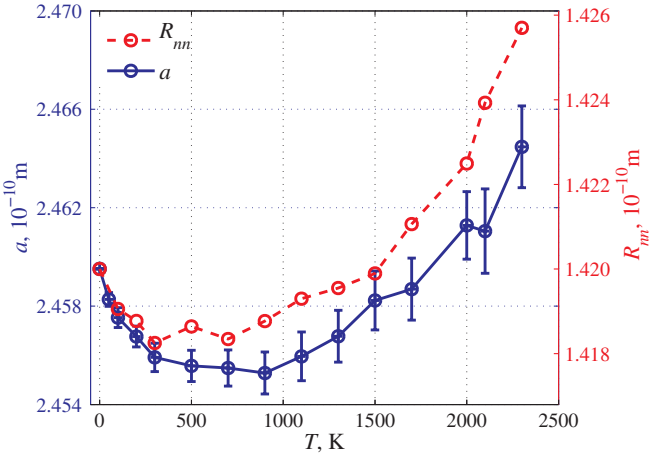

FIG. 1 (color online). Temperature dependence of the lattice parameter a (solid blue line) and nearest neighbor distance R_{nn} (dashed red line). The scales of left (a) and right (R_{nn}) y axes are related to each other by $\sqrt{3}$. At $T = 0$, $a = 2.4595 \times 10^{-10}$ m.

are in agreement up to 500 K with those of Mounet and Marzari [23], who used the quasiharmonic approximation with phonon frequencies and Grüneisen parameters calculated by the density functional approach. However, at higher temperatures our results are qualitatively different, since in Ref. [23] α remains negative in the whole studied temperature interval up to 2200 K, whereas we find that it changes sign and becomes positive at $T \approx 900$ K. This discrepancy with the quasiharmonic theory, which in general works reasonably well for three-dimensional crystals, is one of the evidences of strong anharmonicity in graphene.

The deviations from harmonic behavior can be characterized by examining the radial distribution function $g(R)$ around the first neighbor distance $R_{nn} = 1.42 \times 10^{-10}$ m. In Fig. 2(a), we present $g(R)$ and the related standard deviation $\sigma(R_{nn})$ shown in Fig. 2(b). In the harmonic approximation, R_{nn} would have a Gaussian distribution yielding $\sigma(R_{nn}) \propto \sqrt{T}$. Deviations from square root behavior can be observed above 900 K, achieving 10% at 2000 K.

The Lindemann criterion has been shown to apply also in 2D, giving $\sigma(R_{nn}) \approx 0.23 R_{nn}$ at melting [25]. We found $\sigma(R_{nn})/R_{nn} = 0.056$ at $T = 2300$ K, indicating that we are significantly below the melting point. Moreover, the conventional theory of two-dimensional melting relates it to the formation of topological defects [26]. In our simulations, we have not seen any sign of premelting anomalies (formation of vacancies, topological defects, etc.) up to 3500 K [7].

The strong anharmonic behavior of graphene leads also to an unusual temperature dependence of the elastic moduli.

The 2D bulk modulus b is defined by

$$E_{\mathrm{is}} = 2bu_{\mathrm{is}}^2, \tag{1}$$

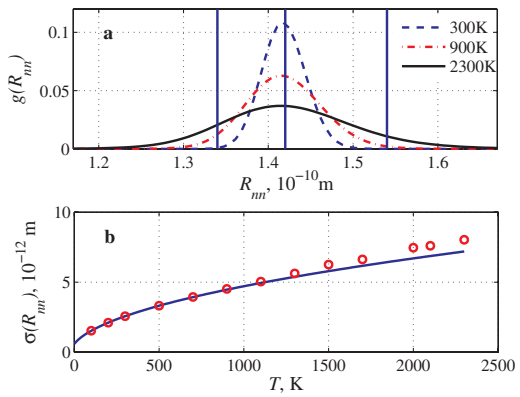

FIG. 2 (color online). (a) Nearest neighbor radial distribution function $g(R_{nn})$ for the $N = 8640$ sample at 300, 900, and 2300 K. The vertical lines indicate the length of double (1.34×10^{-10} m), conjugated (1.42×10^{-10} m), and single (1.54×10^{-10} m) bonds. (b) Standard deviation $\sigma(R_{nn})$ (red circles) and the best fit to $\sqrt{T}$ in the temperature range up to 500 K (solid blue line).

where E_{is} is the elastic energy per unit area under an isotropic deformation $u_{yy} = u_{xx} = u_{\mathrm{is}}$, $u_{xy} = 0$.

For uniaxial deformations u_{xx} ($u_{yy} = u_{xy} = 0$), the elastic energy is

$$E_{\mathrm{uni}} = \tfrac{1}{2}(b + \mu)u_{xx}^2, \tag{2}$$

where μ is the 2D shear modulus.

Isothermal moduli are also expressed as in Eqs. (1) and (2), with replacement of the energy E by the free energy $F = -T \ln Z$, where Z is the partition function. Although it is impossible in MC simulations to calculate F directly, we will use the facts that adiabatic and isothermal shear moduli μ coincide [27] and that the Poisson ratio defined below can be calculated directly to derive the isothermal bulk modulus b_T. The Young modulus Y and Poisson ratio ν are defined in terms of b and μ as [28]

$$Y = \frac{4b\mu}{b + \mu}, \tag{3}$$

$$\nu = \frac{b - \mu}{b + \mu}. \tag{4}$$

The Poisson ratio can also be defined as the ratio between the axial $\epsilon_{\mathrm{axial}}$ and transverse $\epsilon_{\mathrm{trans}}$ strains as

$$\nu = -\frac{\epsilon_{\mathrm{trans}}}{\epsilon_{\mathrm{axial}}}. \tag{5}$$

The latter definition provides a way to calculate the isothermal ν_T so that Eq. (4) with $\mu_A = \mu_T = \mu$ yields b_T.

Adiabatic bulk and shear moduli b_A and μ have been calculated using the following procedure. We equilibrate the sample as described before. Afterwords, 20 configurations separated by 5000 MC steps were stored and subjected to either isotropic or uniaxial deformation in steps of 0.01% without letting the sample relax. For each sample, the variation of the elastic energy with deformation was then fitted to Eq. (1) and (2) over 21 points around the undistorted configuration. The averages of the calculated b_A and μ for the 20 samples are given in Table I and shown in Fig. 3 together with the derived Y_A. We find that the temperature dependence of μ is anomalous. While in general all elastic moduli decrease as a function of temperature due to weakening of interatomic interactions with temperature, in graphene μ grows with increasing temperature up to $T \sim 700$–900 K, which is the same temperature where the thermal expansion behavior (Fig. 1) becomes normal. The Young modulus Y follows the same anomalous temperature dependence as μ.

We find that the behavior of the elastic energy as a function of deformation u is parabolic in a wider range of deformations, up to about 0.2%. For larger deformations, the elastic energies follow a cubic dependence on the deformation at least up to $u = 3\%$. At this value the ratio of the cubic term to the quadratic one in the elastic energy is about 0.12. Up to 10% deformation and up to 2200 K,

TABLE I. Adiabatic bulk (b_A), shear (μ) and isothermal bulk (b_T) moduli, and isothermal Poisson ratio (ν_T).

T, K	b_A (eV · Å^{-2})	μ (eV · Å^{-2})	b_T (eV · Å^{-2})	ν_T
0	12.69	9.44	...	...
100	12.54 ± 0.05	9.57 ± 0.21	13.17 ± 0.98	0.16 ± 0.03
200	12.44 ± 0.03	9.80 ± 0.15	...	...
300	12.36 ± 0.04	9.95 ± 0.17	12.52 ± 1.41	0.12 ± 0.05
500	12.22 ± 0.05	10.16 ± 0.20	12.24 ± 1.66	0.09 ± 0.06
700	12.09 ± 0.05	10.27 ± 0.17	12.93 ± 2.13	0.12 ± 0.08
900	11.94 ± 0.04	10.25 ± 0.18	11.29 ± 2.20	0.09 ± 0.09
1100	11.85 ± 0.06	10.21 ± 0.22	11.31 ± 2.57	0.05 ± 0.11
1300	11.70 ± 0.04	10.07 ± 0.21	12.05 ± 3.00	0.09 ± 0.12
1500	11.57 ± 0.04	9.94 ± 0.18	11.63 ± 3.10	0.08 ± 0.13
1700	11.44 ± 0.04	9.75 ± 0.24	8.44 ± 3.20	−0.07 ± 0.18
2000	11.31 ± 0.06	9.52 ± 0.22	...	...
2100	11.23 ± 0.05	9.46 ± 0.26	8.26 ± 3.58	−0.07 ± 0.21

deformations are reversible, and no defects (vacancy and Stone-Wales [29] or dislocations [30]) are found. This is not surprising in view of the very high cohesive energy (7.37 eV/atom in graphite [22]) of carbon and defect formation energy in graphene [29]. To the best of our knowledge, there are no experimental data on defect formation under strain in this range of temperatures.

Next, the isothermal Poisson ratio ν_T has been calculated using the following procedure. We take the graphene sample equilibrated as described before at a given temperature. The sample is then stretched of 1% in the x and y directions separately and reequilibrated again for at least 5×10^4 MC steps. After reequilibration, the sample size in the x and y directions has been averaged for at least 5×10^4 MC steps, and the corresponding strain ϵ_x and ϵ_y has been calculated yielding the Poisson ratio in each direction through Eq. (5). The Poisson ratios in the x and y directions are very close, and we take their average as ν_T. The calculated adiabatic and isothermal Poisson ratios ν_A and ν_T, respectively, shown in Fig. 4 and Table I, are very small and coincide within the error in the whole studied temperature range. However, at high temperature, we find that ν_T can become negative. Materials with negative Poisson ratio are called auxetic, and, in general, this property is related to very unusual crystalline structures. Membranes, on the other hand, may display this behavior due to entropy. In fact, an expansion in the unstretched direction contrasts the reduction of phase space due to the decrease of height fluctuations due to stretching. Furthermore, the smallness of ν implies that the Lamé constant $\lambda = b - \mu$ is small in comparison with μ. Therefore, for a generic deformation described by a tensor $\hat{u}$, the elastic energy $E_{\rm el} = \mu u_{ij}^2 + (1/2)\lambda u_{ii}^2$ [1] for graphene can be approximated as $E_{\rm el} \approx \mu u_{ij}^2$.

Once ν_T is known, we can calculate b_T from Eq. (4) and Y_T from Eq. (3). The calculated b_T and Y_T are presented in Table I and compared to the adiabatic values in Fig. 3. At $T = 300$ K, we find $Y_A = 353 \pm 4$ N · m^{-1} and $Y_T = 355 \pm 21$ N · m^{-1} in good agreement with the experimental value 340 ± 50 N · m^{-1} [11].

Another important anharmonic effect is the temperature dependence of the molar heat capacity at constant volume $C_V(T) = 3R(1 + T/E_0)$ (see Fig. 5), where R is the gas constant and E_0 is a typical energy of interatomic interactions [13,20]. The low temperature behavior was calculated in the harmonic approximation in Ref. [23]. Our approach is classical and therefore can be used to calculate C_V only at high temperatures, while C_V deviates from $3R$ as T tends to zero. On the other hand, our approach does not use the harmonic approximation, yielding information about phonon-phonon interaction effects. Our calculations show that the linear temperature dependence of C_V becomes noticeable for $T > 800$ K with $E_0 = 1.3$ eV. Contrary to alkali metals where E_0 is of the order of the vacancy formation energy [18], for graphene, due to anharmonicity, E_0 is about 1/5 of the defect formation energy.

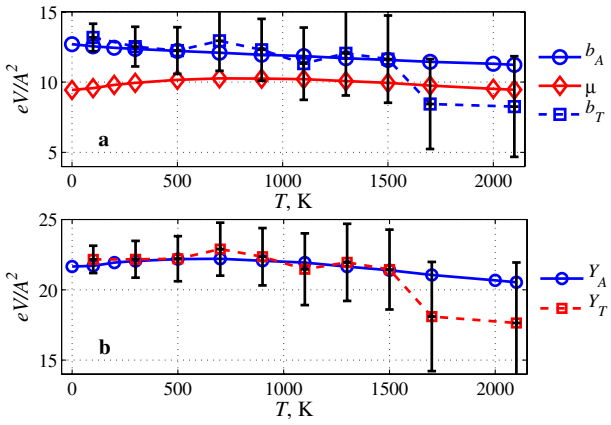

FIG. 3 (color online). (a) 2D elastic moduli of graphene as a function of temperature: adiabatic bulk modulus b_A (solid blue line with circles), isothermal bulk modulus b_T (dashed blue line with squares), and shear modulus μ (solid red line with diamonds). (b) Adiabatic Young's modulus Y_A (solid blue line with circles) and isothermal Y_T (dashed red line with squares).

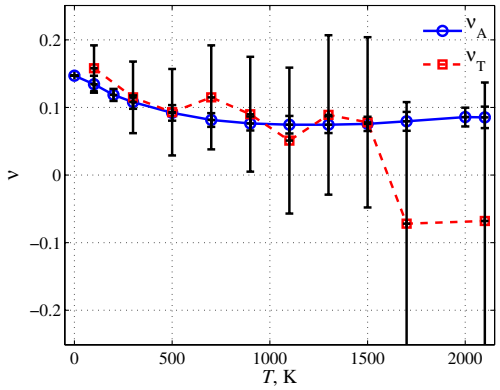

FIG. 4 (color online). Adiabatic ν_A and isothermal ν_T Poisson ratio of graphene as a function of temperature.

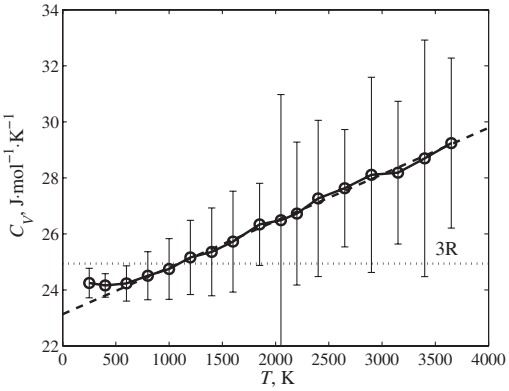

FIG. 5. Temperature dependence of the molar heat capacity at constant volume C_V (solid line) and fit to $C_V(T) = 3R(1 + T/E_0)$ (dashed line).

In summary, we have presented the temperature dependence of the lattice parameter, elastic moduli, and high temperature heat capacity of graphene calculated by Monte Carlo simulations based on the LCBOPII empirical potential [22] for a crystallite of about 15×15 nm^2. In the studied range of temperatures, up to 2200 K, and for a deformation as large as 10% we have not seen any sign of defect formation. Indeed, the very high energy for defect formation in graphene makes this material exceptionally strong, as also found experimentally [11,12]. We find that graphene is strongly anharmonic due to soft bending modes yielding strong out of plane fluctuations. We find that, up to 900 K, graphene is anomalous since its lattice parameter decreases and shear modulus increases with increasing temperature going over to normal behavior at higher temperatures. It would be interesting to check these predictions experimentally.

We thank Jan Los for discussions. This work is part of the research program of the ''Stichting voor Fundamenteel Onderzoek der Materie (FOM),'' which is financially supported by the ''Nederlandse Organisatie voor Wetenschappelijk Onderzoek (NWO).''

[1] *Statistical Mechanics of Membranes and Surfaces*, edited by D. R. Nelson, T. Piran, and S. Weinberg (World Scientific, Singapore, 2004), Chaps. 6 and 11.
[2] K. S. Novoselov, A. K. Geim, S. V. Morozov, D. Jiang, Y. Zhang, S. V. Dubonos, I. V. Grigorieva, and A. A. Firsov, Science **306**, 666 (2004).
[3] A. K. Geim and K. S. Novoselov, Nature Mater. **6**, 183 (2007).
[4] M. I. Katsnelson, Mater. Today **10**, 20 (2007).
[5] A. H. Castro Neto, F. Guinea, N. M. R. Peres, K. S. Novoselov, and A. K. Geim, arXiv:0709.1163 [Rev. Mod. Phy. (to be published)].
[6] Jannik C. Meyer, A. K. Geim, M. I. Katsnelson, K. S. Novoselov, T. J. Booth, and S. Roth, Nature (London) **446**, 60 (2007).
[7] A. Fasolino, J. H. Los, and M. I. Katsnelson, Nature Mater. **6**, 858 (2007).
[8] Eun-Ah Kim and A. H. Castro Neto, Europhys. Lett. **84**, 57007 (2008).
[9] M. I. Katsnelson and A. K. Geim, Phil. Trans. R. Soc. A **366**, 195 (2008).
[10] J. Scott Bunch, Arend M. van der Zande, Scott S. Verbridge, Ian W. Frank, David M. Tanenbaum, Jeevak M. Parpia, Harold G. Craighead, and Paul L. McEuen, Science **315**, 490 (2007).
[11] Changgu Lee, Xiaoding Wei, Jeffrey W. Kysar, and James Hone, Science **321**, 385 (2008).
[12] Tim J. Booth, Peter Blake, Rahul R. Nair, Da Jiang, Ernie W. Hill, Ursel Bangert, Andrew Bleloch, Mhairi Gass, Kostya S. Novoselov, M. I. Katsnelson, and A. K. Geim, Nano Lett. **8**, 2442 (2008).
[13] R. A. Cowley, Adv. Phys. **12**, 421 (1963).
[14] Y. Chen, K. M. Ho, and B. N. Harmon, Phys. Rev. B **37**, 283 (1988).
[15] P. Souvatzis, O. Eriksson, M. I. Katsnelson, and S. P. Rudin, Phys. Rev. Lett. **100**, 095901 (2008).
[16] R. Blinc and B. Zeks, *Ferroelectrics and Antiferroelectrics. Lattice Dynamics* (North-Holland, Amsterdam, 1984).
[17] A. M. Bratkovskii, V. G. Vaks, and A. V. Trefilov, J. Exp. Theor. Phys. **59**, 1245 (1984).
[18] V. G. Vaks, S. P. Kravchuk, and A. V. Trefilov, J. Phys. F **10**, 2105 (1980); **10**, 2375 (1980).
[19] M. Zoli, Phys. Rev. B **41**, 7497 (1990).
[20] M. I. Katsnelson, A. V. Trefilov, M. N. Khlopkin, and K. Yu. Khromov, Philos. Mag. B **81**, 1893 (2001); M. I. Katsnelson, A. F. Maksyutov, and A. V. Trefilov, Phys. Lett. A **295**, 50 (2002).
[21] L. M. Ghiringhelli, J. H. Los, E. J. Meijer, A. Fasolino, and D. Frenkel, Phys. Rev. Lett. **94**, 145701 (2005).
[22] J. H. Los, L. M. Ghiringhelli, E. J. Meijer, and A. Fasolino, Phys. Rev. B **72**, 214102 (2005).
[23] Nicolas Mounet and Nicola Marzari, Phys. Rev. B **71**, 205214 (2005).
[24] M. Lifshitz, Zh. Eksp. Teor. Fiz. **22**, 475 (1952).
[25] F. Lindemann, Phys. Z. **11**, 609 (1910); V. M. Bedanov and G. V. Gadiyak, Phys. Lett. **109A**, 289 (1985); X. H. Zheng and J. C. Earnshaw, Europhys. Lett. **41**, 635 (1998); K. Zahn, R. Lenke, and G. Maret, Phys. Rev. Lett. **82**, 2721 (1999); K. Zahn and G. Maret, *ibid.* **85**, 3656 (2000).
[26] D. R. Nelson and B. I. Halperin, Phys. Rev. B **19**, 2457 (1979).
[27] L. D. Landau and E. M. Lifshitz, *Theory of Elasticity*, Course of Theoretical Physics Vol. 7 (Pergamon, New York, 1959).
[28] P. M. Chaikin and T. C. Lubetsky, *Principles of Condensed Matter Physics* (Cambridge University Press, Cambridge, England, 2003), p. 338.
[29] J. M. Carlsson and M. Scheffler, Phys. Rev. Lett. **96**, 046806 (2006).
[30] A. Carpio, L. L. Bonilla, F. de Juan, and M. A. H. Vozmediano, New J. Phys. **10**, 053021 (2008).